OncoTargets and Therapy

Dovepress
open access to scientific and medical research

Open Access Full Text Article

ORIGINAL RESEARCH

Fabrication of ultrasmall WS_2 quantum dots-coated periodic mesoporous organosilica nanoparticles for intracellular drug delivery and synergistic chemo-photothermal therapy

This article was published in the following Dove Press journal:
OncoTargets and Therapy

Wenyun Liao[1]
Li Zhang[1]
Yunhua Zhong[2]
Yuan Shen[1]
Changlin Li[1]
Na An[1]

[1]Department of Emergency, The First People's Hospital of Yunnan Province, Kunming University of Science and Technology, Kunming, People's Republic of China; [2]Department of Geriatrics, The First People's Hospital of Yunnan Province, Kunming University of Science and Technology, Kunming, People's Republic of China

Introduction: The consolidation of different therapies into a single nanoplatform has shown great promise for synergistic tumor treatment. In this study, a multifunctional platform by WS_2 quantum dots (WQDs)-coated doxorubicin (DOX)-loaded periodic mesoporous organosilicas (PMOs-DOX@WQDs) nanoparticles were fabricated for the first time, and which exhibits good potential for synergistic chemo-photothermal therapy.

Materials and methods: The structure, light-mediated drug release behavior, photothermal effect, and synergistic therapeutic efficiency of PMOs-DOX@WQDs to HCT-116 colon cancer cells were investigated. The thioether-bridged PMOs exhibit a high DOX loading capacity of 66.7 μg mg^{-1}. The gating of the PMOs not only improve the drug loading capacity but also introduce the dual-stimuli-responsive performance. Furthermore, the as-synthesized PMOs-DOX@WQDs nanoparticles can efficiently generate heat to the hyperthermia temperature with near infrared laser irradiation.

Results: It was confirmed that PMOs-DOX@WQDs exhibit remarkable photothermal effect and light-triggered faster release of DOX. More importantly, it was reasonable to attribute the efficient anti-tumor efficiency of PMOs-DOX@WQDs.

Conclusion: The in vitro experimental results confirm that the fabricated nanocarrier exhibits a significant synergistic effect, resulting in a higher efficacy to kill cancer cells. Therefore, the WQD-coated PMOs present promising applications in cancer therapy.

Keywords: periodic mesoporous organosilica, WS_2 quantum dots, chemo-photothermal therapy, drug delivery

Introduction

Cancer is ranked among one of the most severe global health issues,[1] and the global anticancer challenge will be more severe in the next 2 decades.[2] It is urgent to develop new method to defeat this very stubborn disease. Recently, the approach of nanomedicine has provided an outstanding potential to revolutionize tumor treatments.[3–5] Various drug delivery systems have been developed for improvement of therapeutic efficacy and cancer treatment. With the development of material science, pharmaceutical science, and biomedical science, various materials, including polymers, lipids, and inorganic materials have been developed and served as drug carriers to control the release behavior of drugs.[6] Periodic mesoporous organosilicas (PMOs), as one of representative candidate carriers, has attracted great attention in nanomedicine owing to their biocompatibility, high drug-loading capacity, and easily controlled drug release.[7–10] Similar to mesoporous silica nanoparticles (MSN), PMOs nanoparticles,

Correspondence: Li Zhang
Department of Emergency, The First People's Hospital of Yunnan Province, Kunming University of Science and Technology, No. 727 South Jingming Rd., Chenggong District, Kunming, Yunnan 650032, People's Republic of China
Tel/fax +86 871 6363 9921
Email m18302159769@163.com

submit your manuscript | www.dovepress.com
Dovepress
http://dx.doi.org/10.2147/OTT.S160748

which have tunable mesopores that could be utilized for many applications are obtained by the sol–gel process from organo-bridged alkoxysilanes;[11–14] but unlike MSN, the diversity in chemical nature of the pore walls of such nanomaterials is theoretically unlimited.[15] Up to now, various types of PMOs-based stimuli-responsive drug delivery systems have been developed and number of capping agents, such as inorganic nanoparticles, polymers, supramolecular assembles, and biomolecules were used as smart caps on PMOs to control drug release in response to endogenous stimuli.[16–18] Pistone et al prepared the polymer-gated drug delivery systems for smart drug release.[19] Also, Yao et al reported the construction of graphene quantum dots-capped magnetic MSN as a multifunctional platform for synergistic therapy with controlled drug release, magnetic hyperthermia, and photothermal therapy (PTT).[20] Although the controlled drug delivery system could enhance therapeutic efficiency compared with systemic administration,[21] chemotherapy still cannot gain the vintage therapeutic efficacy because the unavoidable multidrug resistance of cancer cells is an inevitable problem.[22–26]

It is generally acknowledged that the purpose of combining two or more therapeutic methodologies is to promote treatment efficacy by integrating the chemotherapy with other therapeutic approaches, such as magnetic hyperthermia, PTT, gene therapy, and radiotherapy.[27–31] Among them, PTT is a promising treatment since it can be controlled spatiotemporally, thus avoiding damage to surrounding healthy tissues.[32] PTT employs photo-absorbing agents, such as gold nanomaterials, organic near-infrared (NIR) dyes, copper chalcogenides, and carbon nanomaterials, to convert optical energy into heat to kill cancer cells.[33–35] Many of recent studies have focused on the combination of PTT and chemotherapy. The integration of PTT and chemotherapy can improve the efficacy of chemotherapeutics and provide an enhanced tailored pharmacological treatment.[36] Therefore, it can be anticipated that the PMOs functionalized with photothermal agents has the potential for controlled drug release, PTT effect, and the improvement of the anticancer performance.

To date, several NIR light-absorbing nanoparticles, which include gold nanorods,[37] graphene nanosheets,[38] carbon dots[39] and many others, inside PMOs has been proposed as a general approach to realize combined PTT and chemotherapy. For example, Chen et al reported a biodegradable nanotheranostics based on copper sulfide-doped periodic mesoporous organosilica nanoparticles with high doxorubicin (DOX)-loading capacity and the DOX release being precisely controllable by triple stimuli and mild hyperthermia-enhanced chemotherapy.[8] Shao et al developed the use of MoS_2 as gatekeepers to cap DOX-loaded periodic mesoporous organosilicas to form a multifunctional platform, which exhibited a great potential for synergistic PTT and chemotherapy.[16]

Recently, a class of two-dimensional (2D) nanomaterials involving MoS_2, WS_2, and Bi_2Se_3 has attracted a significant attention in many fields, which includes nanomedicine applications because of their unique structure, mechanical, electronic, and optical properties.[40–43] WS_2 quantum dots (WQDs) maintain the intrinsic layered structure of graphene but with a smaller lateral size.[44] In addition, by exploiting the high NIR absorbance of WS_2, WQDs can effectively convert NIR light energy into heat, potentially acting as a photothermal agent.[45] Especially, ultrasmall WQDs (<5 nm) can escape the absorption of reticuloendothelial system and could be effectively excreted by kidney rapidly, and thus have the potential for application in biomedicine. The PMOs contain ample thiol bonds, which enable strong binding sites to WQDs. To realize the above purpose, the integration of PMOs and WQDs with drug-loading capacity, stimuli-responsive drug release, and synergistic chemo-PTT for cancer treatment is important.

In this study, we report a solvent exfoliation method strategy to prepare high-quality water-soluble WQDs. The as-prepared WQDs were used as capping agent to construct a novel drug delivery system based on WQDs-coated DOX-loaded periodic mesoporous organosilica (PMOs-DOX@WQDs) for light-mediated drug release. Owing to the hyperthermia-accelerated cellular uptake of nano-carriers and the light-triggered drug release inside cells, synergistic cancer cell killing effect is realized with a combination of photothermal and chemotherapy (Figure 1). Colon cancer line HCT-116 cells were used as model cellular system to evaluate the therapeutic efficiency of the multifunctional platform. The results demonstrated that the PMOs-DOX@WQDs with NIR laser irradiation inhibited cancer cell growth more obviously compared with single treatment, suggesting the synergistic strategy has a great potential in cancer therapy.

Materials and methods

Materials

Tetraethoxysilane (TEOS), cetyltrimethylammonium bromide (CTAB), ethanol, concentrated ammonia aqueous solution ($NH_3 \cdot H_2O$, 25 wt %), concentrated HCl (37%), N-methylpyrrolidone (NMP), and WS_2 powder (99%, <2 μm in size) were purchased from Aladdin Reagent (Shanghai, People's Republic of China). DOX hydrochloride and 1,4-bis(triethoxysily) propane tetrasulfide (TESPTS) were obtained from Sigma-Aldrich (St Louis, MO, USA). Dulbecco's Modified Eagle's Medium (DMEM), PBS, fetal bovine serum (FBS), dimethyl sulfoxide (DMSO), and penicillin–streptomycin solution were obtained from Thermo Fisher

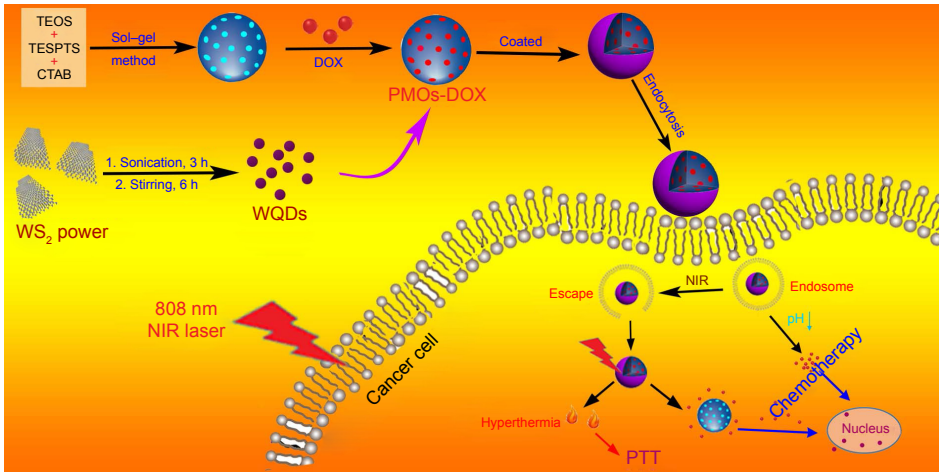

Figure 1 Schematic illustration of the preparation process of the PMOs-DOX@WQDs drug delivery system and synergistic chemo-photothermal therapy.
Abbreviations: CTAB, cetyltrimethylammonium bromide; DOX, doxorubicin; NIR, near-infrared; PMOs, periodic mesoporous organosilicas; PTT, photothermal therapy; TEOS, tetraethoxysilane; TESPTS, 1,4-bis(triethoxysily) propane tetrasulfide; WQDs, WS_2 quantum dots.

Scientific (Waltham, MA, USA). 3-(4,5-Dimethylthiazol-2-yl)-2,5-diphenyltetrazolium bromide (MTT) was purchased from Shanghai Pumai Biotechnology Co. Ltd (Shanghai, People's Republic of China. 4′-6-diamidino-2-phenylindole (DAPI) was purchased from Nanjing Keygen Biotech Co. Ltd. (Nanjing, People's Republic of China). The HCT-116 human colon carcinoma cell line was obtained from KeyGEN Bio TECH Co., Ltd (Nanjing, People's Republic of China). Deionized water (H_2O) was purified by a Millipore system (Milli-Q, 18.2 MΩ cm). All chemicals were of analytical reagent grade and used without further purification.

Synthesis of thioether-bridged PMOs

Thioether-bridged PMOs were synthesized using a sol–gel process according to the previously reported method with some modifications.[46] CTAB (0.12 g) was dissolved in a solution containing concentrated ammonia aqueous solution (1.1 mL, 25 wt %), ethanol (30 mL), and water (80 mL). After the mixture was heated to 35°C for 1 h, TEOS (0.2 mL) and TESPTS (0.1 mL) were mixed and added to the mixture under stirring. The solution was stirred for 24 h at 35°C, and then the product was collected by centrifugation and washed with water and ethanol several times. Finally, the product was redispersed in 150 mL of ethanol and 300 µL of concentrated HCl at 60°C for 3 h to remove the CTAB surfactants. This step was repeated thrice to ensure complete removal of CTAB. The thioether-bridged PMOs were then obtained after drying in vacuum at 50°C for 12 h.

Preparation of WQDs

WQDs were synthesized using a solvent exfoliation method as described in previous work.[45] In a typical procedure, 1 g of WS_2 powder was dispersed in 100 mL NMP and the mixture was sonicated for 3 h at an output power of 250 W to exfoliate the WS_2 powder. Then, the mixture was transferred to a flask and vigorously stirred for 6 h at 140°C. After being cooled to room temperature naturally, the resulting suspensions were centrifuged for 5 min at 2,000 rpm and for 15 min at 12,000. The brown solid was washed twice with deionized water and dried. Subsequently, the solid was redissolved in glutathione (GSH) solution (1 mg/mL) and aged for 24 h at room temperature to form GSH-protected WQDs.

Synthesis of PMOs@WQDs and PMOs-DOX@WQDs

For the synthesis of PMOs-DOX@WQDs, DOX was loaded into PMOs before the capping of WQDs on it. To load DOX, 20 mg of PMOs was dispersed in 10 mL of 0.5 mg/mL DOX–PBS solution. After stirring at room temperature for 24 h under dark conditions, the PMOs-DOX was collected by centrifugation at 11,000 rpm for 10 min. Then PMOs-DOX was further washed with PBS thrice to remove the free DOX and the precipitates were dried under high vacuum (60°C) for further use. Furthermore, all collected supernatant and washed solution were combined and measured by UV-vis spectrophotometer at 484 nm to calculate the content of unloaded DOX.

To cap WQDs on PMOs-DOX nanoparticles, 20 mg of PMOs-DOX was slowly added into the WQDs-GSH solution (10 mL, 1 mg/mL). After the reaction was incubated at 4°C by agitation overnight under dark conditions, the WQDs capped PMOs-DOX (PMOs-DOX@WQDs) was collected by centrifugation and washed with H_2O to remove the residual WQDs. Finally, the products were lyophilized and

kept at 4°C. Also, PMOs@WQDs were obtained using the same process but without DOX loading.

Characterization

Transmission electron microscopy (TEM) imaging was performed using a Tecnai T12 microscope (FEI Company, Hillsboro, OR, USA). Scanning electron microscopy (SEM) was carried out using an FEI Quanta 450 field emission scanning electron microscope. The X-ray diffraction (XRD) pattern was characterized on a D8 Advance powder X-ray diffractometer (Bruker, Karlsruhe, Germany). N_2 sorption isotherms was measured on a Micromeritics ASAP 2020 M apparatus (Micromeritics Instrument Corp., Norcross, GA, USA). Brunauer–Emmett–Teller and Barrett–Joyner–Halenda methods were used to determine the surface area, pore size distribution, and the pore volume. UV-vis spectra was taken using a Genesys 10S UV-vis spectrophotometer (Thermo Fisher Scientific Inc., Madison, WI, USA). The zeta potential and dynamic light scattering (DLS) were measured on a Malvern Zetasizer Nano-ZS90 (Malvern, UK). The photothermal conversion efficiency was analyzed using a laser device (Shanghai Xilong Optoelectronics Technology Co. Ltd., Shanghai, People's Republic of China) with a wavelength of 808 nm, and the temperature of the solution was tracked using a DT-8891E thermocouple linked to a digital thermometer (Shenzhen Everbest Machinery Industry, Shenzhen, People's Republic of China).

Photothermal effect measurement

Different PMOs concentrations (0, 1, 2.5, 5, 10, and 20 mg/mL) of PMOs-DOX@WQDs in PBS were prepared, and a total volume of 500 μL of each concentration was irradiated by an 808 nm NIR laser for 5 min at 1.0 W/cm^2. Then, the PMOs-DOX@WQDs solution at a concentration of 5 mg mL^{-1} was irradiated with different power densities (0.25, 0.5, 1, and 1.5 W cm^{-2}) over a period of 5 min. As control, the photothermal effect of the PMOs-DOX solution was also measured. Finally, the samples were irradiated for 5 min each time with 5 on-off cycles to detect the thermal stability of PMOs-DOX@WQDs.

In vitro pH and laser-responsive drug release

In vitro pH-responsive DOX release was executed in PBS solution of pH 5 and 7.4. And in vitro laser-responsive DOX releas was conducted in PBS with laser irradiation (808 nm, 1.0 W cm^{-2}) for 10 min. In brief, 10 mg of PMOs-DOX@WQDs were dispersed in PBS (10 mL) at different pH (7.4 and 5.0), which was further shaken at a speed of 100 rpm at 37°C. For laser-triggered drug release, 2 mL of PBS solution at different pH containing PMOs-DOX@WQDs (5 mg/mL PMOs) was irradiated by 808 nm NIR laser irradiation for 10 min. Afterward, the solution was shaken at 100 rpm (37°C) for another 1 h. Then releasing system was centrifuged and the same volume of fresh PBS was appended for continuous drug release. The obtained clear supernatant was used to determine the released drug amount by a UV-vis spectrometer at a wavelength of 484 nm. The control group was performed with identical conditions but was without irradiation.

Cell culture

HCT-116 cells were cultured in DMEM, supplemented with 10% FBS and 1% antibiotics (1,000 U/mL of penicillin and 1,000 μg/mL of streptomycin). The cells were maintained at 37°C with 5% CO_2 atmosphere and the culture medium was changed every 2 days. Because this cell line is adherent, non-coated round glass coverslips were sterilized in 70% ethanol and then placed at the bottom of the wells before adding cells and the media.

In vitro cytotoxicity assay

The cytotoxicity of PMOs@WQDs on HCT-116 cells was determined by MTT assay. The cells were seeded in 96-well plates at a density of 1×10^4 cells/well and incubated for 24 h. Then the medium was removed and replaced with 100 μL of fresh medium that contained PMOs@WQDs at different concentrations, and incubated for another 24 h at 37°C. Then 10 μL of MTT (5 mg/mL in PBS, pH 7.4) was added to each well and the plate was incubated at 37°C for another 4 h. Then the culture medium was removed and DMSO (150 μL) was added to each well for dissolving the formazan crystals. Finally, the absorbance of the solution was determined at 570 nm using a microplate reader (BioTek Instruments, Winooski, VT, USA). The cell viability was calculated according to the formula: OD (test cells)/OD (reference cells) ×100%.

In vitro cellular uptake of PMOs-DOX@WQDs

To investigate cell uptake of the PMOs-DOX@WQDs nanoparticles, HCT-116 cells were seeded at a density of 1×10^5 cells/well in a 35-mm glass-base dish overnight. After washing the cells with PBS twice, the complete culture medium was replaced with PMOs-DOX@WQDs (100 μg/mL), and then incubated at 37°C for 4 h. In addition, another group treated with PMOs-DOX@WQDs was exposed to laser irradiation at a power density of 1.0 W/cm^2 for 5 min after 2 h incubation. After a total of 4 h incubation,

1 mL of methanolic solution of DAPI (1.5 μg/mL) was added into the Petri dish and incubated at 37°C for 15 min to stain the nuclei. Subsequently, the cells were gently washed with PBS thrice and observed by using a Carl Zeiss LSM 700 laser scanning confocal microscope (Jena, Germany).

In vitro chemo-photothermal therapy

The HCT-116 cells were cultured in 96-well plates at a density of 1×10^4 cells per well and incubated for 24 h. Then the cells were washed with PBS twice, and the medium was replaced with 100 μL of fresh DMEM containing PMOs@WQDs, free DOX, and PMOs-DOX@WQDs at different concentrations. For laser irradiation group, certain groups of cells were exposed to 1.0 W/cm^2 laser irradiation for 5 min after 2 h incubation. As control, HCT-116 cells were without any treatment. After 24 h incubation, the cells were washed with PBS and then MTT solution (5 mg/mL in PBS, 10 μL) was added to each well, and further incubated for 4 h at 37°C to measure cell viability.

Statistical analysis

Data were expressed as mean ± SD. The difference was determined by Student's *t*-test and $P<0.05$ was considered statistically significant. Statistical analysis of the data was performed using SPSS 17.0 (SPSS Inc., Chicago, IL, USA).

Results and discussion

Preparation and characterization of the PMOs-DOX@WQDs nanoparticles

PMOs with thioether-bridged structure were synthesized by a CTAB-directed sol–gel process. SEM and TEM images of the PMOs are shown in Figure 2A and B. They exhibit a spherical shape and a uniform diameter of about 100 nm. The XRD pattern of the PMOs nanoparticles shows a strong peak at 2.59°, which suggests the PMOs have an ordered mesostructure (Figure S1). N_2 isorption results of PMOs in Figure 3 exhibits type IV isotherm characteristics, which proved that PMOs maintain a mesoporous structure. The surface area and pore diameter of the PMOs were calculated to be as high as 1,055 m^2 g^{-1} and 3.78 nm, respectively.

The WQDs was synthesized via solvent exfoliation method strategy. GSH was used as surfactant to control the size and stabilize the yielded products. A typical TEM image of the resultant WQDs shows that the WQDs are well dispersed with a narrow lateral size distribution and the average diameter is

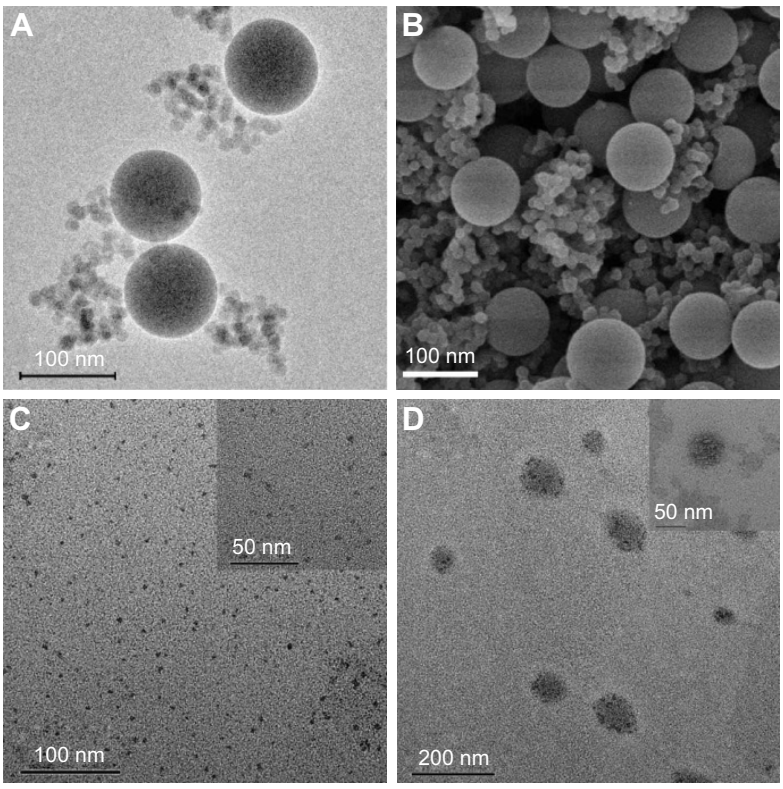

Figure 2 (**A**) TEM and (**B**) SEM image of the thioether-bridged PMOs. (**C**) TEM images of WQDs synthesized via bottom-up method and (**D**) TEM images of PMOs-DOX@WQDs.
Notes: The magnification of these images was ×60,000 for (**A** and **B**), ×50,000 for (**C**), ×25,000 for (**D**), and ×100,000 for the insert of (**C** and **D**).
Abbreviations: DOX, doxorubicin; PMOs, periodic mesoporous organosilicas; SEM, scanning electron microscopy; TEM, transmission electron microscopy; WQDs, WS_2 quantum dots.

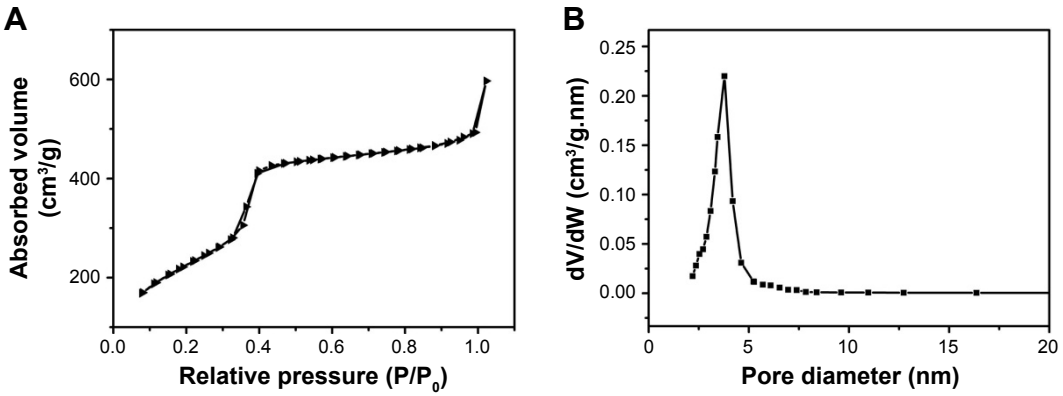

Figure 3 (**A**) Nitrogen adsorption–desorption isotherms for PMOs and (**B**) the corresponding pore size distributions.
Abbreviation: PMOs, periodic mesoporous organosilicas.

about 2.8 nm (Figure 2C and inset of Figure 2C). Figure S2 shows the Raman spectrum of the WQDs, and 2 Raman peaks can be observed at 378.6 and 437.2 cm^{-1}, corresponding to the in-plane (E^1_{2g}) and out-of-plane (A_{1g}) vibrations of the W−S bonds in 2H-WS_2. The difference of those 2 peaks is about 58.6 cm^{-1}, demonstrating the thin-layer structure of the WQDs.

After loading DOX, WQDs are used as the capping agent to cap the outlets of mesoporous channels for the formation of the PMOs-DOX@WQDs nanoparticles, which can prevent the DOX from leaking. It should be noted that TEM did not clearly show a spherical shape, but the existing mesopores were observed (inset in Figure 2D) and WQDs were grafted on the surfaces of the nanoparticles to block the mesopores (Figure 2D). The content of WQDs in PMOs-DOX@WQDs was further measured by ICP-AES analysis (Varian 710-ES, Varian Medical Systems, Palo Alto, CA, USA), indicating 114 μg mg^{-1} of PMOs. Importantly, DLS measurements indicated that the average particle size of PMOs and PMOs-DOX@WQDs are 219 and 256 nm, respectively (Figure 4A), which suggests a thin-layer structure of the WQDs. The result is well in accordance with the TEM and Raman results. We further evaluated the colloidal stability of the PMOs-DOX@WQDs by dispersing the nanoparticles in water, PBS, and cell culture medium for 1 month (Figure 4B). It can be seen that the particles do not aggregate at room temperature. The stability of the PMOs-DOX@WQDs dispersed in PBS was further checked by DLS (insert in Figure 4B). It was shown that the hydrodynamic size of the particles does not change significantly for at least 1 week. Zeta potentials were further used to characterize the preparation process and WQDs wrapping of PMOs-DOX (Figure 4C). The zeta potential of PMOs is negative, around 38.6 mV, which turned to 29.4 mV when loaded with DOX because of negatively charged DOX. Upon subsequent capping of negative WQDs (−45.6 mV), a negative value of −18.4 mV was obtained for PMOs-DOX@WQDs, which further confirmed the successful loading of DOX and the coating of WQDs.

UV-vis spectra was used to further confirm the formation of the PMOs-DOX@WQDs. As shown in Figure 4D, the absorbance peak at 481 nm for PMOs-DOX and PMOs-DOX@WQDs is attributed to the characteristic absorbance of DOX, which suggests the DOX loading. Meanwhile, the absorption peaks demonstrate the successful wrapping of WQDs around the PMO-DOX. Furthermore, the DOX-loading capacity of the PMOs@WQDs was also measured to be 66.7 μg mg^{-1} PMOs by UV-vis analysis according to the different DOX concentration between the initial solution and the residual supernatant (Figure S3).

Photothermal effect of the PMOs-DOX@WQDs nanoparticles

Similar to 2D WS_2 nanosheets, the WQDs fabricated by the hydrothermal method also showed relative high absorbance in the NIR region (Figure 4D). Capping with WQDs endows the PMOs-DOX@WQDs with photothermal performance upon NIR irradiation. To investigate the photothermal effect of the PMOs-DOX@WQDs, different concentrations of PMOs-DOX@WQDs were irradiated by NIR 808 nm laser irradiation at power density of 1 W/cm^2 for 5 min. As shown in Figure 5A, the temperature only slightly increased in pure H_2O, but increased with increasing concentration of PMOs-DOX@WQDs in the suspension by NIR irradiation, which confirms the photothermal effect for the PMOs-DOX@WQDs. For example, the temperature can be increased from 25.6°C to 55.9°C with 5 min irradiation at a PMOs concentration of 10 mg mL^{-1}. On the other hand, 2.5 mg/mL of PMOs in PMOs-DOX@WQDs was exposed to 808 nm laser irradiation with different power densities and the results

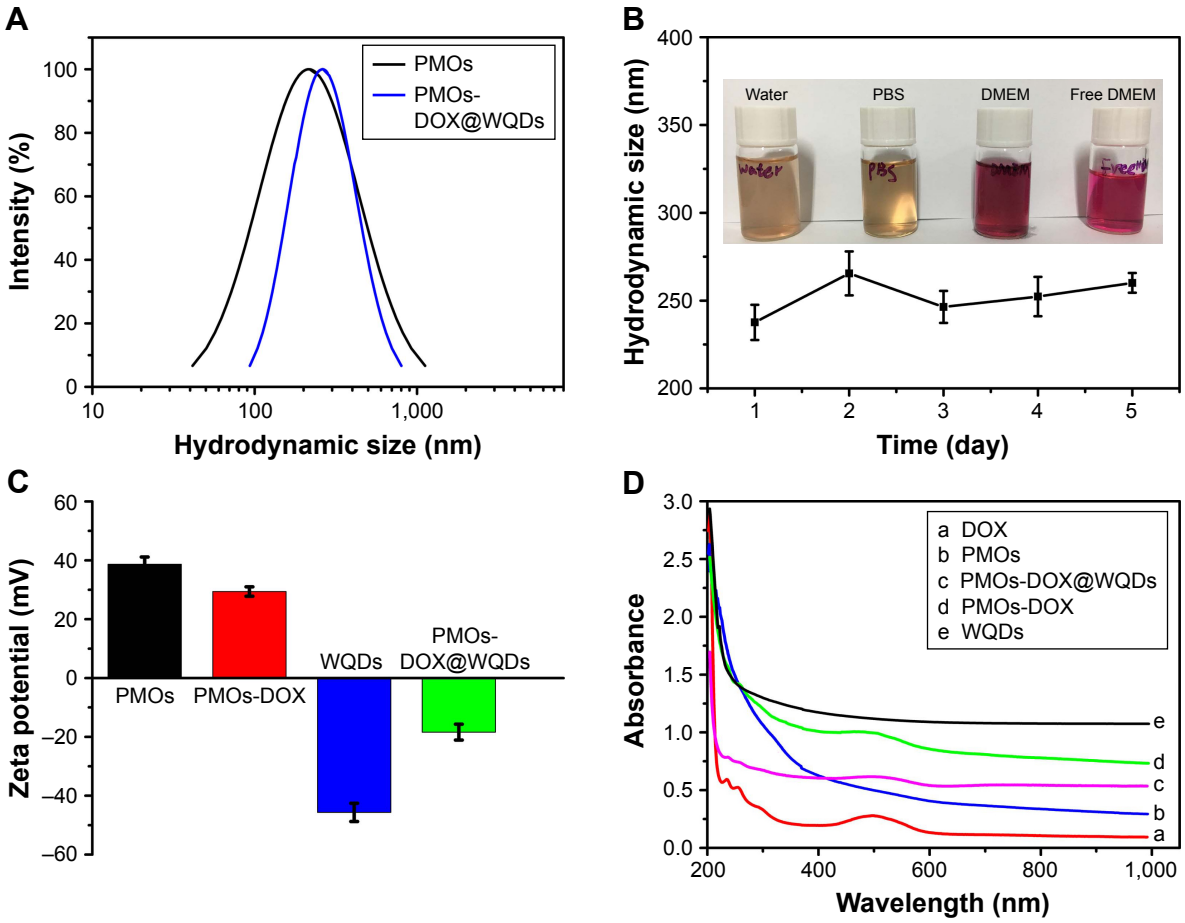

Figure 4 (**A**) Hydrodynamic diameters of the PMOs, PMOs-DOX@WQDs. (**B**) Hydrodynamic size of PMOs-DOX@WQDs dispersed in different solutions for 5 days. Inset of (**B**) The photograph of PMOs dispersed in water, PBS, and DMEM. (**C**) Zeta potentials of PMOs, PMOs-DOX, WQDs, and PMO-DOX@WQDs. (**D**) UV-vis absorption spectra of DOX, PMOs, PMOs-DOX, WQDs, and PMOs-DOX@WQDs nanoparticles.

Abbreviations: DMEM, Dulbecco's Modified Eagle's Medium; DOX, doxorubicin; PMOs, periodic mesoporous organosilicas; WQDs, WS_2 quantum dots.

show a laser power-dependent photothermal effect and the temperature up to 53.9°C at a power density of 1.5 W cm^{-2} for 5 min (Figure 5B). Meanwhile, PMOs-DOX@WQDs show an excellent photothermal stability within 5 cycles of laser irradiation (Figure 5C), which suggests that PMOs-DOX@WQDs is a promising potent agent for PTT.

In vitro drug release

To evaluate the drug-release behavior in response to pH and NIR laser irradiation, the in vitro drug release profiles of PMOs-DOX@WQDs were investigated in pH 7.4 or 5.0 buffer solution, followed with or without the NIR laser irradiation, respectively. Figure 5D shows the cumulative DOX release from the PMOs-DOX@WQDs under different conditions. Take pH 5.0 as an example, the cumulative release of DOX (67.5%) with NIR irradiation was about 1.5-fold greater than without NIR irradiation (45%). These results indicate that the photothermal effect of the WQDs can efficiently trigger the release of DOX from the nanocarrier. It might be related to the decrease of electrostatic interaction between DOX and PMOs. Meanwhile, the PMOs-DOX@WQDs exhibited a pH-responsive pattern, whereas a higher cumulative DOX release was achieved in relation to a lower pH (pH=5.0). The phenomenon can be attributed to the decrease of interaction between WQDs and PMOs nanoparticles under acidic conditions, resulting in the easy dissociation of WQDs from the PMOs-DOX@WQDs nanoparticles. Meanwhile, at low pH, the reduced electrostatic attraction between PMOs and DOX was attributed to the protonation effect of more surface silanols, thus leading to DOX release. Therefore, it is evident that the pH-sensitive and NIR-stimulative release of DOX can greatly enhance the delivery efficiency and therapeutic effect.

In vitro cytotoxicity and cell uptake of the PMOs-DOX@WQDs nanoparticles

In this study, in vitro cytotoxicity of the PMOs@WQDs nanoparticles was investigated by MTT assay to evaluate

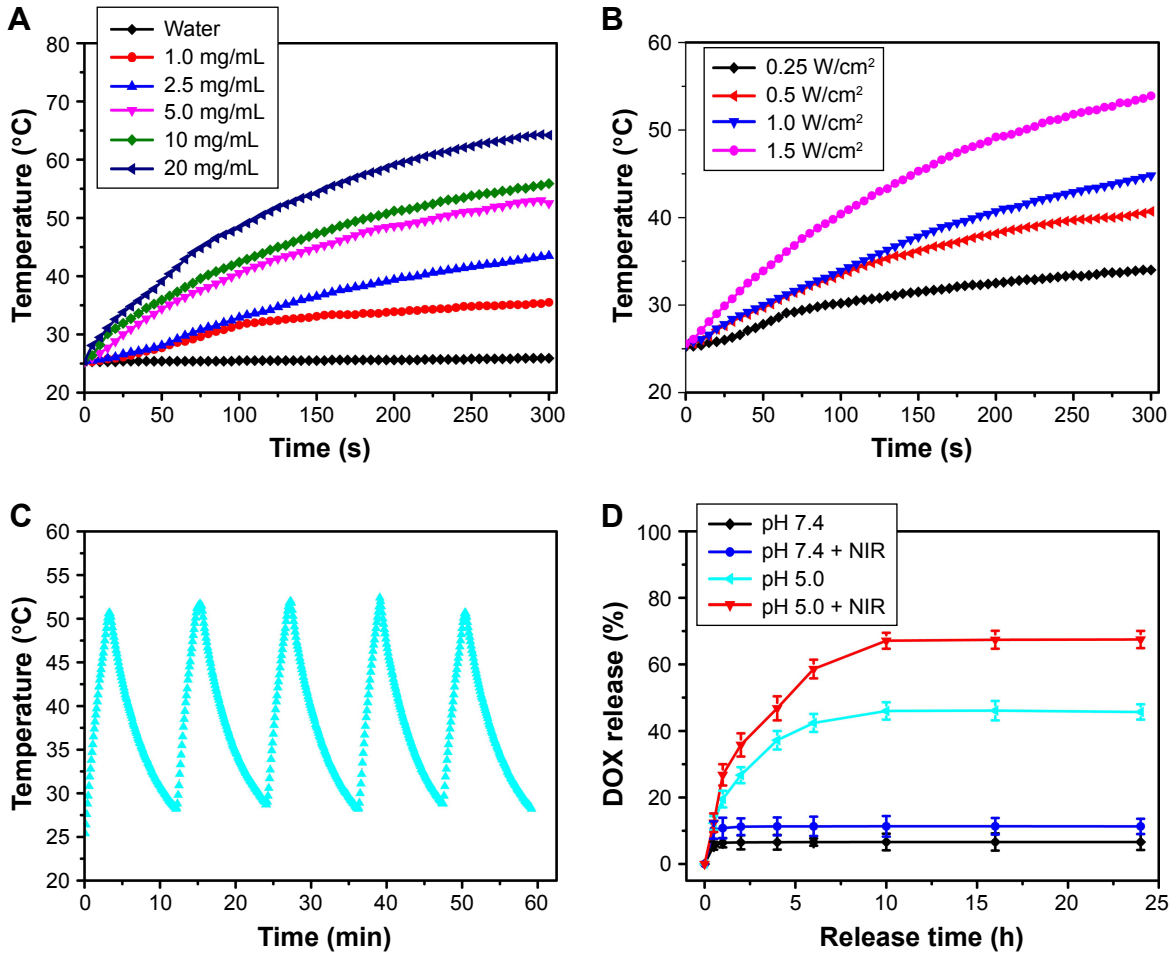

Figure 5 (**A**) Photothermal heating curves of H_2O and PMOs-DOX@WQDs suspension with different concentrations. (**B**) Photothermal heating curves of PMOs-DOX@WQDs (equivalent concentration is 5 mg mL^{-1}) at different laser power densities for 5 min. (**C**) Plot of temperature of the aqueous solution containing the PMOs-DOX@WQDs as a function of time (laser on for 300 s for each cycle, and laser off) for 5 cycles. (**D**) DOX release profiles from PMOs-DOX@WQDs nanocomposites at different pH with or without NIR laser irradiation.

Abbreviations: DOX, doxorubicin; NIR, organic near-infrared; PMOs, periodic mesoporous organosilicas; WQDs, WS_2 quantum dots.

biological safety and biocompatibility of nanocarriers. As shown in Figure 6, after incubation of HCT-116 cells with the PMOs@WQDs for 24 h, the relative viability remained above 89% with concentrations from 0 to 200 μg/mL, indicating no cytotoxicity for the PMOs@WQDs nanoparticles.

The detailed cellular uptake and intracellular NIR-photoresponsive drug release of the PMOs-DOX@WQDs was monitored by confocal microscopy images. As shown in Figure 7A, a red fluorescence signal from the DOX molecules was observed in the nuclei in every group, which was attributed to DOX release from the PMOs-DOX@WQDs. Meanwhile, strong red fluorescence was observed inside the nuclei of NIR irradiation group, which was significantly higher than the without NIR group. The results confirmed that mild hyperthermia not only enhanced the cell uptake of PMOs-DOX@WQDs but could also trigger the release of DOX.

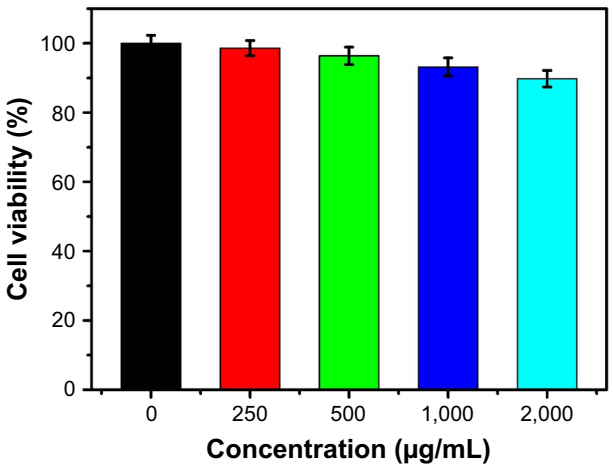

Figure 6 Cell viabilities of the HCT-116 cells after incubation with different concentrations of PMOs@WQDs as measured by MTT assay.

Abbreviations: HCT, human colon cancer; MTT, 3-(4,5-Dimethylthiazol-2-yl)-2,5-diphenyltetrazolium bromide; PMOs, periodic mesoporous organosilicas; WQDs, WS_2 quantum dots.

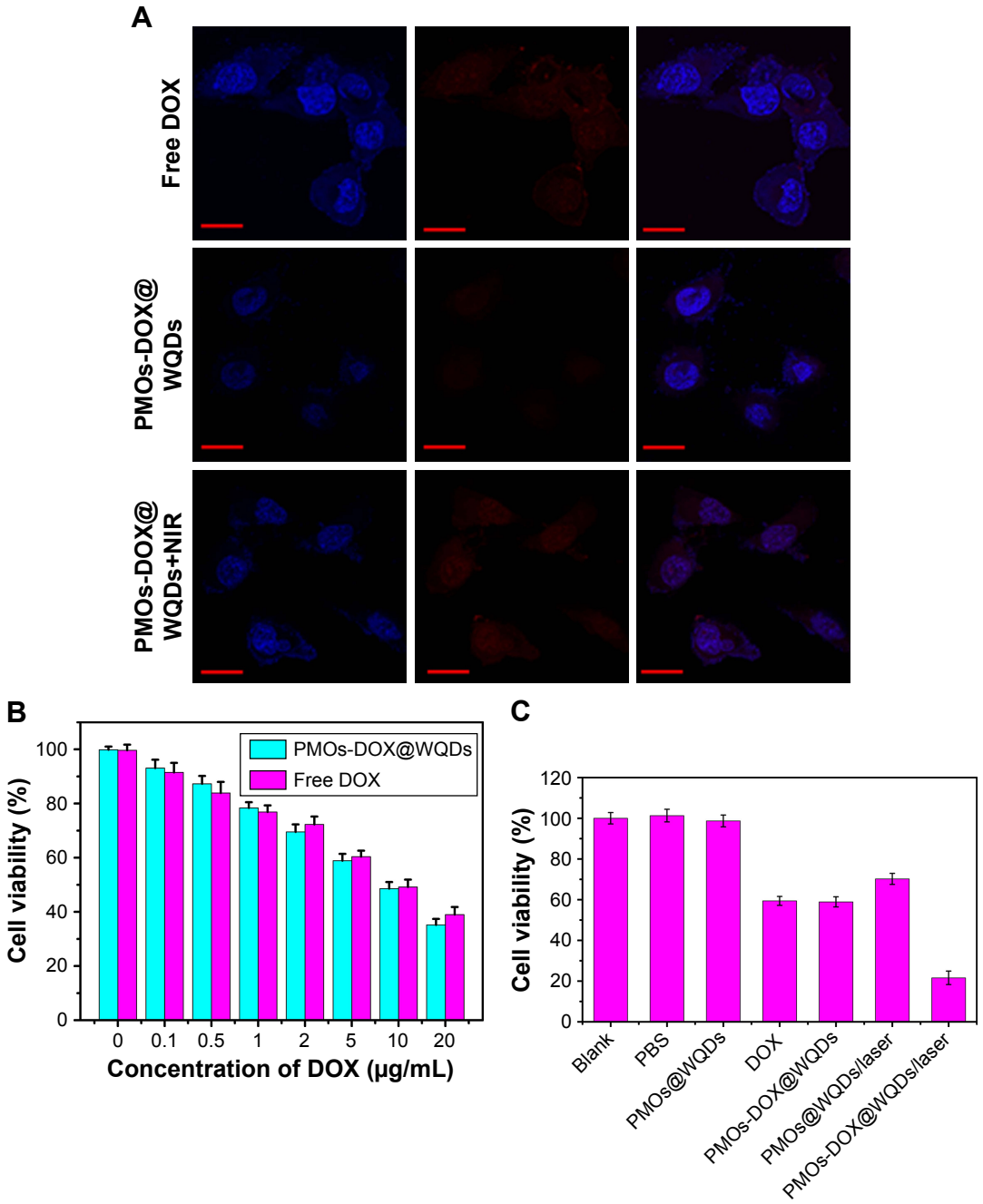

Figure 7 (**A**) CLSM of the HCT-116 cells after 8 h incubation with free DOX, PMOs-DOX@WQDs only, PMOs@WQDs with laser irradiation and PMOs-DOX@WQDs with laser irradiation (relative DOX concentration: 10 μg/mL) Scale bar: 50 μm; magnification: ×40. (**B**) Cell viability of HCT-116 cells incubated with different concentrations of DOX and PMOs-DOX@WQDs (equivalent concentration of DOX). (**C**) Cell viability of HCT-116 after 8 h incubation with PBS, free DOX, PMOs@WQDs, and PMOs-DOX@WQDs suspensions (DOX: 5.0 μg/mL) with and without NIR irradiation.

Abbreviations: CLSM, confocal microscopy images; DOX, doxorubicin; HCT, human colon cancer; NIR, near infrared; PMOs, periodic mesoporous organosilicas; WQDs, WS_2 quantum dots.

Therefore, the fabricated nanoplatform shows great potential for synergistic chemo-photothermal therapy.

In vitro chemo-photothermal therapy

The in vitro synergistic effect of chemo-PTT was evaluated by MTT assay after different treatments. As shown in Figure 7B, with equivalent doses of DOX, the free DOX and PMOs-DOX@WQDs nanocomposites exhibited similar cytotoxicity on HCT-116 cells and reflected a dose-dependence. Meanwhile, the group exposed to chemo-PTT (PMOs-DOX@WQDs/laser) possessed stronger inhibition efficiency than chemotherapy (PMOs-DOX@WQDs and

free DOX) and PTT (PMOs@WQDs/laser) alone, regardless of drug concentrations (Figure 7C). For instance, when the HCT-116 cells was treated with the highest drug concentration (5 μg/mL of DOX) and NIR laser irradiation (1.0 W cm^{-2}, 5 min), the relative cell viabilities decreased significantly (21.6%), and were remarkably lower than those treated with PMOs-DOX@WQDs alone (59%) or PMOs@WQDs with NIR irradiation (70.2%), indicating the excellent therapeutic efficiency of the synergistic effect of PMOs-DOX@WQDs plus NIR irradiation on cancer cells. Furthermore, it should be pointed out that the single chemotherapy efficiency of the PMOs-DOX@WQDs nanoparticles was slightly lower compared to free DOX at the same DOX concentration, which may be attributed to the fact that DOX was released from the PMOs-DOX@WQDs nanoparticles after cell uptake, resulting in lower DOX concentration in cells owing to the partial internalization of the PMOs-DOX@WQDs nanoparticles in cells within the experiment period.[20] However, the combination of the chemotherapy with PTT could achieve the synergistic effect to kill cancer cells efficiently. Therefore, the PMOs-DOX@WQDs nanoparticles exhibited potential for drug-controlled release and PTT.

Conclusion

In summary, we have reported a multifunctional platform based on WQDs-coated thioether-bridged PMOs nanoparticles for synergistic therapy with controlled drug release and PTT for the first time. The WQDs were synthesized via a simple solvent exfoliation process, and the internal mesopores cavity of PMOs was found to be ideal for loading anti-cancer drug DOX. The as-prepared PMOs-DOX@WQDs exhibits excellent drug-loading ability, good biocompatibility, and photothermal ability. The loaded DOX shows a significant pH and NIR-responsive release by laser irradiation and acidic environment. Using the HCT-116 tumor cells as a cellular system, we found that PMOs@WQDs were internalized by the cells and had negligible cytotoxicity. Importantly, the in vitro investigations confirmed that PMOs-DOX@WQDs nanoparticles could efficiently deliver DOX to HCT-116 tumor cells and presented an excellent synergistic chemo-PTT effect. Therefore, this system provides new inspiration for the construction of a stimuli-responsive drug delivery system and holds great promise for improving the therapeutic efficiency of cancer therapy.

Acknowledgments

This research was financially supported by the project of Science and Technology Commission of Yunnan Province (No 2017FE467).

Disclosure

The authors report no conflicts of interest in this work.

References

1. Chen D, Dougherty CA, Zhu K, Hong H. Theranostic applications of carbon nanomaterials in cancer: focus on imaging and cargo delivery. *J Control Release*. 2015;210:230–245.
2. McGuire S. World cancer report 2014. Geneva, Switzerland: World Health Organization, International Agency for Research on Cancer, WHO Press, 2015. *Adv Nutr*. 2016;7(2):418–419.
3. Luo Z, Hu Y, Cai K, et al. Intracellular redox-activated anticancer drug delivery by functionalized hollow mesoporous silica nanoreservoirs with tumor specificity. *Biomaterials*. 2014;35(27):7951–7962.
4. Shi J, Kantoff PW, Wooster R, Farokhzad OC. Cancer nanomedicine: progress, challenges and opportunities. *Nat Rev Cancer*. 2017;17(1):20–37.
5. Wong PT, Choi SK. Mechanisms of drug release in nanotherapeutic delivery systems. *Chem Rev*. 2015;115(9):3388–3432.
6. Liu D, Yang F, Xiong F, Gu N. The smart drug delivery system and its clinical potential. *Theranostics*. 2016;6(9):1306–1323.
7. Lu N, Tian Y, Tian W, et al. Smart cancer cell targeting imaging and drug delivery system by systematically engineering periodic mesoporous organosilica nanoparticles. *ACS Appl Mater Interfaces*. 2016;8(5):2985–2993.
8. Lu N, Huang P, Fan W, et al. Tri-stimuli-responsive biodegradable theranostics for mild hyperthermia enhanced chemotherapy. *Biomaterials*. 2017;126:39–48.
9. Teng Z, Su X, Zheng Y, et al. A facile multi-interface transformation approach to monodisperse multiple-shelled periodic mesoporous organosilica hollow spheres. *J Am Chem Soc*. 2015;137(24):7935–7944.
10. Chen Y, Meng Q, Wu M, et al. Hollow mesoporous organosilica nanoparticles: a generic intelligent framework-hybridization approach for biomedicine. *J Am Chem Soc*. 2014;136(46):16326–16334.
11. Croissant JG, Cattoen X, Wong MC, Durand JO, Khashab NM. Syntheses and applications of periodic mesoporous organosilica nanoparticles. *Nanoscale*. 2015;7(4):20318–20334.
12. Waki M, Mizoshita N, Tani T, Inagaki S. Periodic mesoporous organosilica derivatives bearing a high density of metal complexes on pore surfaces. *Angew Chem Int Ed Engl*. 2011;50:11667–11671.
13. Tani T, Mizoshita N, Inagaki S. Luminescent periodic mesoporous organosilicas. *J Mater Chem*. 2009;19:4451–4456.
14. Mizoshita N, Tani T, Shinokubo H, Inagaki S. Mesoporous organosilica hybrids consisting of silica-wrapped π-π stacking columns. *Angew Chem Int Ed Engl*. 2012;51(5):1156–1160.
15. Lin D, Hu L, You H, Tolbert SH, Loy DA. Comparison of new periodic, mesoporous, hexylene-bridged polysilsesquioxanes with *Pm3n* symmetry versus sol–gel polymerized, hexylene-bridged gels. *J Non-Cryst Solids*. 2014;406:139–143.
16. Shao T, Wen J, Zhang Q, et al. NIR photoresponsive drug delivery and synergistic chemo-photothermal therapy by monodispersed-MoS_2-nanosheets wrapped periodic mesoporous organosilicas. *J Mater Chem B*. 2016;4:7708–7717.
17. Jiao J, Liu C, Li X, et al. Fluorescent carbon dot modified mesoporous silica nanocarriers for redox-responsive controlled drug delivery and bioimaging. *J Colloid Interface Sci*. 2016;483:343–352.
18. Lei Q, Qiu WX, Hu JJ, et al. Multifunctional mesoporous silica nanoparticles with thermal-responsive gatekeeper for NIR light-triggered chemo/photothermal therapy. *Small*. 2016;12(31):4286–4298.
19. Alessandro P, Daniela I, Shabana A, et al. Tunable doxorubicin release from polymer-gated multiwalled carbon nanotubes. *Int J Pharm*. 2016;515(1–2):30–36.
20. Yao X, Niu X, Ma K, et al. Graphene quantum dots-capped magnetic mesoporous silica nanoparticles as a multifunctional platform for controlled drug delivery, magnetic hyperthermia, and photothermal therapy. *Small*. 2017;13(2):1602225–1602236.
21. Yao X, Tian Z, Liu J, Zhu Y, Hanagata N. Mesoporous silica nanoparticles capped with graphene quantum dots for potential chemo-photothermal synergistic cancer therapy. *Langmuir*. 2017;33(2):591–599.

22. Im JH, Seong J, Lee IJ, et al. Surgery alone versus surgery followed by chemotherapy and radiotherapy in resected extrahepatic bile duct cancer: treatment outcome analysis of 336 patients. *Cancer Res Treat*. 2016;48(2):583–595.
23. Liu J, Detrembleur C, De Pauw-Gillet MC, Mornet S, Jérôme C, Duguet E. Gold nanorods coated with mesoporous silica shell as drug delivery system for remote near infrared light-activated release and potential phototherapy. *Small*. 2015;11(9):2323–2332.
24. Yhee JY, Song S, Lee SJ, et al. Cancer-targeted MDR-1 siRNA delivery using self-cross-linked glycol chitosan nanoparticles to overcome drug resistance. *J Control Release*. 2015;198:1–9.
25. Zhu H, Chen H, Zeng X, et al. Co-delivery of chemotherapeutic drugs with vitamin ETPGS by porous PLGA nanoparticles for enhanced chemotherapy against multi-drug resistance. *Biomaterials*. 2014;35(7):2391–2400.
26. Tian G, Zheng X, Zhang X, et al. TPGS-stabilized $NaYbF_4$:Er upconversion nanoparticles for dual-modal fluorescent/CT imaging and anticancer drug delivery to overcome multi-drug resistance. *Biomaterials*. 2015;40:107–116.
27. Wang Y, Gu H. Core-shell-type magnetic mesoporous silica nanocomposites for bioimaging and therapeutic agent delivery. *Adv Mater*. 2015;27(3):576–585.
28. Kong L, Xing L, Zhou B, Du L, Shi X. Dendrimer-modified MoS_2 nanoflakes as a platform for combinational gene silencing and photothermal therapy of tumors. *ACS Appl Mater Interfaces*. 2017;9(19):15995–16005.
29. Kou Z, Wang X, Yuan R, et al. A promising gene delivery system developed from PEGylated MoS_2 nanosheets for gene therapy. *Nanoscale Res Lett*. 2014;9(1):587.
30. Luo L, Bian Y, Liu Y, et al. Combined near infrared photothermal therapy and chemotherapy using gold nanoshells coated liposomes to enhance antitumor effect. *Small*. 2016;12(30):4103–4112.
31. He L, Lai H, Chen T. Dual-function nanosystem for synergetic cancer chemo-radiotherapy through ROS-mediated signaling pathways. *Biomaterials*. 2015;51:30–42.
32. Jaque D, Martínez Maestro L, del Rosal B, et al. Nanoparticles for photothermal therapies. *Nanoscale*. 2014;6:9494–9530.
33. Cheng X, Sun R, Yin L, Chai Z, Shi H, Gao M. Light-triggered assembly of gold nanoparticles for photothermal therapy and photoacoustic imaging of tumors in vivo. *Adv Mater*. 2016;29(6):1604894–1604900.
34. Chen Q, Liu X, Zeng J, Cheng Z, Liu Z. Albumin-NIR dye self-assembled nanoparticles for photoacoustic pH imaging and pH-responsive photothermal therapy effective for large tumors. *Biomaterials*. 2016;98:23–30.
35. Wang L, Shi J, Jia X, et al. NIR-/pH-Responsive drug delivery of functionalized single-walled carbon nanotubes for potential application in cancer chemo-photothermal therapy. *Pharm Res*. 2013;30(11):2757–2771.
36. Wu J, Liu Y, Tang Y, et al. Synergistic chemo-photothermal therapy of breast cancer by mesenchymal stem cell-encapsulated yolk-shell GNR@HPMO-PTX nanospheres. *ACS Appl Mater Interfaces*. 2016;8(28):17927–17935.
37. Hu H, Liu J, Yu J, et al. Synthesis of Janus Au@periodic mesoporous organosilica (PMO) nanostructures with precisely controllable morphology: a seed-shape defined growth mechanism. *Nanoscale*. 2017;9(14):4826–4834.
38. He D, He X, Wang K, Zou Z, Yang X, Li X. Remote-controlled drug release from graphene oxide-capped mesoporous silica to cancer cells by photoinduced pH-jump activation. *Langmuir*. 2014;30(24):7182–7189.
39. Lei J, Yang L, Lu D, et al. Carbon dot-incorporated PMO nanoparticles as versatile platforms for the design of ratiometric sensors, multichannel traceable drug delivery vehicles, and efficient photocatalysts. *Adv Opt Mater*. 2015;3(1):57–63.
40. Chou SS, Kaehr B, Kim J, et al. Chemically exfoliated MoS_2 as near-infrared photothermal agents. *Angew Chem Int Ed Engl*. 2013;52(15):4160–4164.
41. Chen Y, Wang L, Shi J. Two-dimensional non-carbonaceous materials-enabled efficient photothermal cancer therapy. *Nano Today*. 2016;11(3):292–308.
42. Tan L, Wang S, Xu K, et al. Layered MoS_2 hollow spheres for highly-efficient photothermal therapy of rabbit liver orthotopic transplantation tumors. *Small*. 2016;12(15):2046–2055.
43. Wang S, Li K, Chen Y, et al. Biocompatible PEGylated MoS_2 nanosheets: controllable bottom-up synthesis and highly efficient photothermal regression of tumor. *Biomaterials*. 2015;39:206–217.
44. Dong H, Tang S, Hao Y, et al. Fluorescent MoS_2 quantum dots: ultrasonic preparation, up-conversion and down-conversion bioimaging, and photodynamic therapy. *ACS Appl Mater Interfaces*. 2016;8(5):3107–3114.
45. Xu S, Li D, Wu P. One-Pot, facile, and versatile synthesis of monolayer MoS_2/WS_2 quantum dots as bioimaging probes and efficient electrocatalysts for hydrogen evolution reaction. *Adv Funct Mater*. 2015;25(7):1127–1136.
46. Wang T, Guan B, Wang X, et al. Mesostructured TiO_2 gated periodic mesoporous organosilica-based nanotablets for multistimuli-responsive drug release. *Small*. 2015;11(44):5907–5911.

Supplementary materials

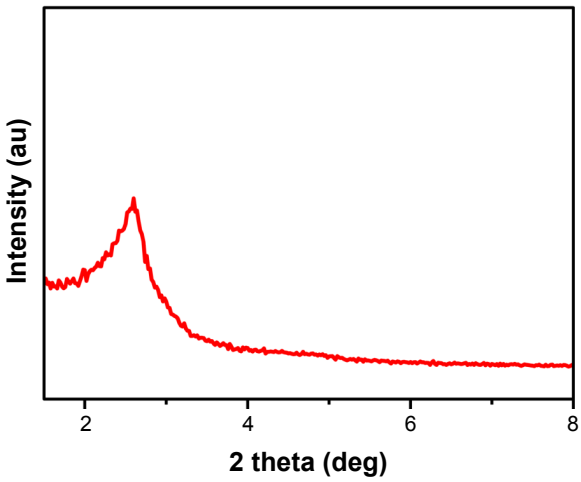

Figure S1 XRD pattern of the thioether-bridged PMOs synthesized by a CTAB-directed sol–gel method.
Abbreviations: CTAB, cetyltrimethylammonium bromide; PMOs, periodic mesoporous organosilica; XRD, X-ray diffraction.

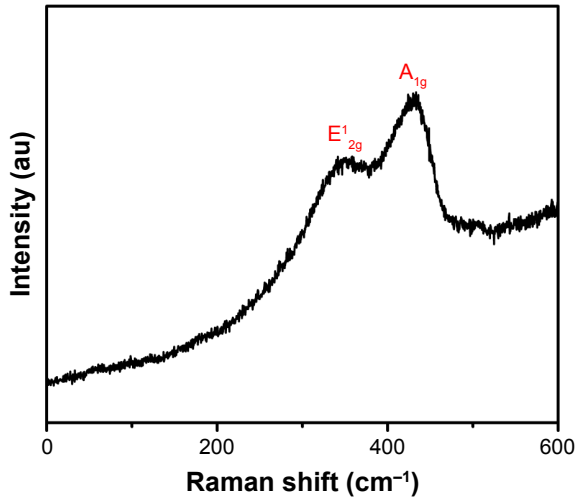

Figure S2 Raman spectra of the WQDs (Ex: 535 nm).
Abbreviation: WQDs, WS_2 quantum dots.

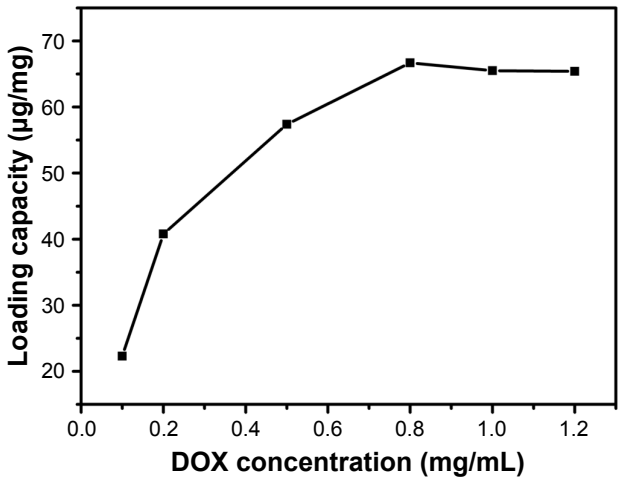

Figure S3 The DOX-loading capacities on PMOs@WQDs with different DOX concentrations.
Abbreviations: DOX, doxorubicin; PMOs, periodic mesoporous organosilica; WQDs, WS_2 quantum dots.